J. Plasma Phys. (2024), *vol*. 90, 905900508
Published by Cambridge University Press.
doi:10.1017/S002237782400117X

Reinterpreting radio frequency heating and current drive theory in a tokamak

Peter J. Catto †

Plasma Science and Fusion Center, Massachusetts Institute of Technology, Cambridge, MA 02139, USA

(Received 13 February 2024; revised 29 August 2024; accepted 2 September 2024)

Quasilinear treatments are widely used for tokamaks to evaluate radio frequency (rf) heating and current drive. Even though the core of a tokamak plasma is weakly collisional, the solution of the linearized kinetic equation is evaluated using unperturbed collisionless trajectories while often treating successive poloidal circuits of the passing (and trapped) particles as uncorrelated or nearly so. In addition, the most important effect of tokamak geometry, the mirror force, is usually mistreated or ignored when obtaining the solution. These concerning aspects of rf treatments are clarified by considering lower hybrid heating and current drive to illustrate that the electrons in resonance with the applied rf are enclosed by narrow collisional boundary layers, and that tokamak geometry makes it necessary to retain poloidal variation when solving a weakly collisional linearized kinetic equation. Other aspects such as collisional boundary layers at the trapped–passing boundary, cyclotron resonances, and the limitations of quasilinear theory are also considered. The new insights lead to a fundamentally different formulation and interpretation of the solution of the linearized Fokker–Planck equation used for rf quasilinear theory in a tokamak, while retaining many of the features that have contributed to its successful application to rf heating and current drive.

Keywords: fusion plasma, plasma heating, plasma waves

1. Introduction

Some of the complications of treatments of radio frequency (rf) heating and current drive are removed by considering the linearized electron response to an applied, steady state rf wave with a frequency ω well below the electron cyclotron frequency Ω (species subscripts are suppressed for notational simplicity since only electrons are considered). The application to this lower hybrid (Bonoli 2014) and helicon (Prater *et al.* 2014) regime allows the linearized and quasilinear physics issues to be illustrated in a tractable manner, but is extendable to other frequency ranges. The physics focus is on the combined role of retaining the enhanced sensitivity to collisions of the resonant electrons and the impact of properly treating tokamak geometry. One or both of these phenomena are ignored or incompletely treated in full wave formulations of heating and current drive such as AORSA (Jaeger *et al.* 2001, 2006, 2008), TorLH (Wright *et al.* 2009), LHEAF (Meneghini, Shiraiwa & Parker 2009; Shiraiwa *et al.* 2010), KINETIC-J (Green & Berry 2014), and TORIC (Brambilla & Bilato 2020) that are based on collisionless,

† Email address for correspondence: catto@psfc.mit.edu

homogeneous or otherwise inadequate treatments of magnetic field variation in the linearized kinetic equation. In these descriptions the mirror force is typically ignored, simplified or mistreated when solving the linearized kinetic equation. Moreover, any memory of a preceding resonant wave–particle interaction is normally assumed lost from one poloidal circuit to the next (Stix 1975, 1992; Bernstein & Baxter 1981; Kasilov, Pyatak & Stepanov 1990; Lamalle 1993, 1997). In addition, the quasilinear operator derived in a homogeneous magnetic field (Kennel & Engelmann 1966) is typically allowed to have spatial variation, which then leads to an improper transit or bounce averaged quasilinear operator (Petrov & Harvey 2016) with incorrect spatial behaviour. Often a stationary phase (or higher order Airy) expansion that assumes successive passes through resonance are uncorrelated (Bernstein & Baxter 1981; Kasilov *et al.* 1990; Lee *et al.* 2018) is employed even though the fusion plasmas in the core of a tokamak are only weakly collisional. Except in Belikov & Kolesnichenko (1994), these procedures implicitly and incorrectly treat tokamak geometry in the linear kinetic response, and therefore in the quasilinear operator as well, as shown by Catto & Tolman (2021*a*).

The enhanced role of collisions in the linearized kinetic equation is due to the formation of narrow collisional boundary layers in velocity space surrounding and broadening the resonant particle trajectories. Collisions are the only physical process that can be retained that maintains the linearity of the perturbed kinetic equation, as required for a quasilinear formulation. In addition, a realistic treatment of tokamak geometry must account for the strong and important poloidal variation of the parallel velocity $v_{||}$ that is responsible for the presence of trapped and passing particles (Belikov & Kolesnichenko 1982, 1994; Catto & Tolman 2021*a*) that respond very differently to the applied rf field and result in behaviour that is not captured by near homogenous (or quasilocal eikonal) linearized treatments. Furthermore, the long mean free path nature of collisions means that successive poloidal circuits for the passing and bounces for the trapped electrons are well correlated. As a result, the linearized resonant electron response must be consistent with a transit averaged resonance condition on the unperturbed orbits, rather than the spatially localized one normally employed. The transit averaged resonance condition appearing in the linear solution of the kinetic equation is then consistent with the one appearing in the quasilinear operator derived by Catto & Tolman (2021*a*) in the presence of collisions.

Certain aspects of these issues are addressed in earlier publications which consider resonant particle collisions in a uniform plasma (Catto 2020; Catto & Tolman 2021*b*) and a full gyrokinetic treatment of rf heating and current drive in a tokamak (Catto & Tolman 2021*a*) as well as the evaluation of lower hybrid and helicon current drive, in tokamak geometry (Catto 2021; Catto & Zhou 2023). Here, however, the task is to expand on how some of these earlier results can be put to use to find a sensible non-singular solution to the linearized electron kinetic equation that accounts for both the presence of collisional boundary layers and tokamak geometry. Even though an exact analytic solution is not possible in the most general case considered, it is possible to find what is expected to be a remarkably good, non-singular analytic solution. The procedures employed allow the coupling of poloidal modes to be treated in a streamlined fashion and then extended further to include the collisional boundary layers associated with the resonant electrons. In addition, insights into the collisional boundary layers that must exist at the trapped–passing boundary are possible. The weakly collisional linearized results remove the singular behaviour of the delta function at the transit average resonance that enters in the quasilinear operator of Catto & Tolman (2021*a*). The diffusive nature of pitch angle scattering collisions is responsible for the existence of narrow boundary layers enclosing the electrons experiencing wave–particle resonances. The existence of these

https://doi.org/10.1017/S002237782400117X Published online by Cambridge University Press

resonances allows collisions to enter to resolve singular behaviour in the solutions of the linearized kinetic equation.

Tokamak geometry means that the parallel velocity $v_{||}$ of an electron slows as it moves into a higher field magnetic field region and, depending on its magnetic moment, leads to the existence of trapped as well as passing electrons. In addition, in a weakly collisional tokamak plasma the poloidal angle dependence of the parallel velocity and the gyrofrequency results in the coupling of many poloidal mode numbers m for each toroidal mode number n. This geometrical effect is essential to retain since many poloidal modes can contribute. Using the parallel velocity as an independent variable does not avoid these issues since then the mirror force term must be retained to capture the full effects of tokamak geometry.

The presence of trapped and passing electrons and diffusive pitch angle scattering collisions also means that there are collisional boundary layers at the trapped–passing boundary where these distribution functions must vanish. Otherwise, the differing phase-space responses to the rf do not allow them to match even in a piecewise continuous manner.

The section that follows gives a brief derivation of the electron kinetic equation for lower hybrid and helicon waves, followed by a concise section on collisional boundary layers without geometrical complications. Section 4 reviews the wave–particle resonance condition for electrons in a large aspect ratio tokamak. It is followed by a treatment in § 5 of collisional boundary layers in tokamaks without the complication of poloidal mode coupling. Poloidal mode coupling is then treated in tokamak geometry using a Krook collision model in § 6. Section 7 uses the earlier results to construct a plausible (but non-rigorous) collisional boundary layer solution that retains poloidal mode coupling. The collisional boundary layers associated with the trapped–passing boundary are considered in § 8. In § 9 extensions of the collisional boundary layer treatments and tokamak geometry effects to cyclotron resonances are briefly mentioned. Section 10 discusses the compatibility of the results found here with those of Catto & Tolman (2021*a*), while § 11 demonstrates how to obtain improved expressions for the perturbed density and currents. The limitations of quasilinear theory are addressed in § 12, followed by a discussion section.

2. Electron kinetic equation

Consider an applied low frequency rf wave of frequency $\omega \ll \varOmega = eB/mc$ in an axisymmetric tokamak magnetic field

$$\boldsymbol{B} = B\boldsymbol{n} = I\nabla\zeta + \nabla\zeta \times \nabla\psi, \tag{2.1}$$

with B the magnitude of the magnetic field, $\boldsymbol{n}$ the unit vector in the magnetic field direction, ζ the toroidal angle variable, ψ the poloidal flux function, $I = I(\psi) = RB_t$ with R the major radius and B_t the toroidal magnetic field, m and e the mass and magnitude of the charge on an electron and c the speed of light. Then for a lowest order Maxwellian distribution function

$$f_0 = n(m/2T)^{3/2}\,\mathrm{e}^{-mv^2/2T}, \tag{2.2}$$

quasilinear rf treatments solve the linearized electron kinetic equation

$$-\mathrm{i}\omega f_1 + \boldsymbol{v}\boldsymbol{\cdot}\nabla f_1 - \varOmega\boldsymbol{v}\times\boldsymbol{n}\boldsymbol{\cdot}\nabla_v f_1 - C\{f_1\} = -(e/T)\boldsymbol{e}\boldsymbol{\cdot}\boldsymbol{v}f_0, \tag{2.3}$$

using unperturbed particle trajectories. Here, C is the electron collision operator, $\boldsymbol{e} \propto \mathrm{e}^{-\mathrm{i}\omega t}$ is the applied rf field, $f_1 \propto \mathrm{e}^{-\mathrm{i}\omega t}$ is the perturbed electron distribution function, $\varOmega = eB/mc$

https://doi.org/10.1017/S002237782400117X Published online by Cambridge University Press

is the electron cyclotron frequency and T is the electron temperature. To simplify the presentation the unperturbed electric field is neglected, and only a single applied frequency ω and toroidal mode number n are considered.

The gyrokinetic variables (Catto 1978, 2019) $E = v^2/2$ (kinetic energy), $\mu = v_\perp^2/2B$ (magnetic moment), $\varphi =$ gyrophase and $\boldsymbol{R} = \boldsymbol{r} - \varOmega^{-1}\boldsymbol{v} \times \boldsymbol{n}$ (guiding centre location) are used to derive the electron kinetic equation, with $\boldsymbol{v} = \boldsymbol{v}_\perp + v_{||}\boldsymbol{n}$, $v_{||}^2 = v^2 - 2\mu B$, $\boldsymbol{v}_\perp = v_\perp(\boldsymbol{e}_\psi \cos\varphi + \boldsymbol{e}_\times \sin\varphi)$, and the orthonormal unit vectors satisfying $\boldsymbol{n} = \boldsymbol{e}_\psi \times \boldsymbol{e}_\times$, where $\boldsymbol{e}_\psi = \nabla\psi/|\nabla\psi| = \nabla\psi/RB_p$. The poloidal magnetic field B_p is assumed positive, making $B_t > 0$ for co-current operation and $B_t < 0$ when operation is counter-current.

To lowest order, $\partial f_1/\partial\varphi = 0$ in the lower hybrid and helicon wave limit of interest. Gyroaveraging the next order equation holding $\boldsymbol{R}$ fixed, and Fourier decomposing by writing

$$\boldsymbol{e} = \Sigma_m \boldsymbol{e}_m\, \mathrm{e}^{\mathrm{i}n\zeta - \mathrm{i}m\vartheta + \mathrm{i}S(\psi) - \mathrm{i}\omega t} = \mathrm{e}^{\mathrm{i}n\zeta - \mathrm{i}\omega t}\Sigma_m \boldsymbol{e}_m\, \mathrm{e}^{-\mathrm{i}m\vartheta + \mathrm{i}S(\psi)}, \tag{2.4}$$

leads to (Catto 2020; Catto & Tolman 2021*a*)

$$-\mathrm{i}\omega f_1 + (\mathrm{i}qnf_1 + \partial f_1/\partial\vartheta)v_{||}\boldsymbol{n}\cdot\nabla\vartheta - C\{f_1\} = \Sigma_m W_m\, \mathrm{e}^{-\mathrm{i}m\vartheta}, \tag{2.5}$$

with $f_1 \propto \mathrm{e}^{\mathrm{i}n\zeta - \mathrm{i}\omega t}$ to streamline the notation and

$$W_m = -(e/T)[\boldsymbol{e}_m\cdot\boldsymbol{n}\, J_0(\eta)v_{||} + \mathrm{i}k_\perp^{-1}v_\perp \boldsymbol{e}_m\cdot\boldsymbol{k}\times\boldsymbol{n}\, J_1(\eta)]f_0\, \mathrm{e}^{-\mathrm{i}L}, \tag{2.6}$$

where $\boldsymbol{k} = \nabla S(\psi) - m\nabla\vartheta + n\nabla\zeta$, $k_{||} = (qn - m)\boldsymbol{n}\cdot\nabla\vartheta \approx (qn - m)/qR$, $\eta = k_\perp v_\perp/\varOmega$ and the poloidal angle ϑ defined such that $q = q(\psi) = |I(\psi)|/R^2\boldsymbol{B}\cdot\nabla\vartheta$. To find the preceding, write $\boldsymbol{k}_\perp = k_\perp(\boldsymbol{e}_\psi\cos\beta + \boldsymbol{e}_\times\sin\beta)$, $L = \varOmega^{-1}\boldsymbol{k}\cdot\boldsymbol{v}\times\boldsymbol{n} = \eta\sin(\varphi - \beta)$, and $\mathrm{e}^{-\mathrm{i}L} = \Sigma_p\, \mathrm{e}^{-\mathrm{i}p(\varphi-\beta)}J_p(\eta)$ to obtain $(2\pi)^{-1}\oint \mathrm{d}\varphi\, \mathrm{e}^{\mathrm{i}L} = J_0(\eta)$ and $(2\pi)^{-1}\oint \mathrm{d}\varphi\ \mathrm{e}^{\mathrm{i}L}\boldsymbol{v}_\perp = -\mathrm{i}k_\perp^{-1}v_\perp\boldsymbol{k}\times\boldsymbol{n}J_1(\eta)$. The result is similar to that of a homogenous plasma, where it corresponds to using $\mathrm{e}^{\mathrm{i}\boldsymbol{k}\cdot\boldsymbol{r}} = \mathrm{e}^{\mathrm{i}\boldsymbol{k}\cdot\boldsymbol{R}+\mathrm{i}L}$ prior to gyroaveraging at fixed $\boldsymbol{R}$. Additional Bessel functions will appear when the density and current are formed as they are evaluated in $\boldsymbol{r}$ and $\boldsymbol{v}$ variables, requiring $\boldsymbol{R} = \boldsymbol{r} - \varOmega^{-1}\boldsymbol{v}\times\boldsymbol{n}$ to be employed once again. To streamline the notation the $\mathrm{e}^{-\mathrm{i}L}$ factor that results from this change back is displayed in W_m since the distinction between $\boldsymbol{r}$ and $\boldsymbol{R}$ is unimportant elsewhere in the kinetic equation. As time evolution and the departure from axisymmetry do not result in any temporal or toroidal mode coupling, a monochromatic wave is considered.

The narrow boundary layers that must be considered are assumed to be due to pitch angle scattering collisions of parallel streaming for a couple of reasons. First, pitch angle scattering dominates for collisional boundary layers at a trapped–passing boundary at large aspect ratio. Second, for lower hybrid heating (Bonoli 2014) and lower hybrid and helicon current drive (Catto & Zhou 2023), a high-speed expansion of the electron–electron collision operator is normally adequate and tends to make energy scatter less important. Consequently, the replacement

$$C\{f_1\} \to \frac{2\nu_e B_0\xi}{Bx^3}\frac{\partial}{\partial\lambda}\left(\lambda\xi\frac{\partial f_1}{\partial\lambda}\right), \tag{2.7}$$

is normally adequate, where $\nu_e = 3\sqrt{\pi}(Z+1)\nu_{ee}/4$, $\nu_{ee} = 4\sqrt{2\pi}e^4 n\ell n\varLambda_C/3m^{1/2}T^{3/2}$, $x = v/v_e$, $v_e = (2T/m)^{1/2}$ is the electron thermal speed, and $\ell n\varLambda_C$ is the Coulomb logarithm. In addition, $v_{||}^2 = v^2\xi^2 = v^2 - 2\mu B = v^2(1 - \lambda B/B_0)$, with B_0 a flux function at most. When lower hybrid heating and current drive due to lower hybrid and helicon waves is evaluated, the second or energy scatter term appearing in (4.2) of Catto & Zhou (2023) is required (unfortunately, the x^3 is missing in the denominator of their first term)

https://doi.org/10.1017/S002237782400117X Published online by Cambridge University Press

since when the collision operator acts on f_0, instead of f_1, there are no boundary layers in the f_0 equation.

When the linearized kinetic equation is solved numerically it may be convenient to use v and $v_{||}$ variables. Then, the $\mu \boldsymbol{n}\cdot\nabla B$ mirror force term explicitly appears in the equation

$$-\mathrm{i}\omega f_1 + \left(\mathrm{i}qnf_1 + \frac{\partial f_1}{\partial\vartheta}\right) v_{||}\boldsymbol{n}\cdot\nabla\vartheta - \mu\boldsymbol{n}\cdot\nabla B\frac{\partial f_1}{\partial v_{||}} - \frac{\nu_e}{2x^3}\frac{\partial}{\partial v_{||}}\left[(v^2 - v_{||}^2)\frac{\partial f_1}{\partial v_{||}}\right] = \Sigma_m W_m\,\mathrm{e}^{-\mathrm{i}m\vartheta}. \tag{2.8}$$

In v and μ variables the mirror force is implicit in the ϑ variation of $v_{||}^2 = v^2(1-\lambda B/B_0)$.

3. Collisional boundary layer for resonant electrons without geometrical effects

In a cylindrical plasma immersed in a homogenous magnetic field B_0, $v_{||}^2 = v^2(1-\lambda) = v^2\xi^2$. It is then convenient to use v, $v_{||}$ as velocity variables in place of v, λ as there is no poloidal mode coupling or mirror force. The kinetic equation is then simply

$$-\mathrm{i}(\omega - k_{||}v_{||})f_m - \bar{\nu}(v)\frac{\partial}{\partial v_{||}}\left(v_\perp^2\frac{\partial f_m}{\partial v_{||}}\right) = W_m, \tag{3.1}$$

for $f_1 = \mathrm{e}^{\mathrm{i}n\zeta - \mathrm{i}\omega t}\Sigma_m f_m\,\mathrm{e}^{-\mathrm{i}m\vartheta+\mathrm{i}S}$ and where $\bar{\nu}(v) = 2\nu_e/x^3$. To see that a narrow collisional boundary layer of width $\Delta v_{||}$ arises when $k_{||}\neq 0$, the estimates $k_{||}v_{||} - \omega = k_{||}\Delta v_{||}$ and $\partial/\partial v_{||}\sim 1/\Delta v_{||}$ are used to balance the resonance term with collisions, $k_{||}\Delta v_{||}\sim\bar{\nu}v_\perp^2/(\Delta v_{||})^2\equiv\bar{\nu}_{\mathrm{eff}}$, to obtain $\Delta v_{||}/v_e\sim(\bar{\nu}v_\perp^2/k_{||}v_e^3)^{1/3}\sim(\bar{\nu}/k_{||}v_e)^{1/3}\ll 1$ and the effective collision frequency $\bar{\nu}_{\mathrm{eff}}\sim\bar{\nu}(k_{||}^2v_\perp^2/\bar{\nu}^2)^{1/3}\gg\bar{\nu}$. Consequently, the resonant electrons are in a collisionally broadened boundary layer, and have a wave–particle interaction time of $\bar{\tau}_{\mathrm{int}} = 1/\bar{\nu}_{\mathrm{eff}}$. Since the mean free path of an electron is $\sim v_e/\nu_e\sim 10^4$ metres, for $1/k_{||}\sim 10$ metres, this gives $\Delta v_{||}/v_e\sim 1/10$, $\bar{\nu}_{\mathrm{eff}}/\bar{\nu}\sim 100$, and a resonant electron mean free path of $v_e\bar{\tau}_{\mathrm{int}}\sim 100$ metres.

To see this more rigorously, Catto (2020) uses the narrowness of the boundary layer in $v_{||}$ space to ignore the $v_{||}$ dependence of $v_\perp^2 = v^2 - v_{||}^2$. Then, introducing the new variable

$$s = (k_{||}v_{||}-\omega)/(k_{||}^2v_\perp^2\bar{\nu})^{1/3}, \tag{3.2}$$

finds the non-singular solution

$$f_m = \frac{W_m}{(k_{||}^2v_\perp^2\bar{\nu})^{1/3}}\int_0^\infty \mathrm{d}t\,\mathrm{e}^{-\mathrm{i}st-t^3/3} \underset{s\to\pm\infty}{\rightarrow} \frac{-W_m}{\mathrm{i}(\omega - k_{||}v_{||})} \rightarrow W_m\pi\delta(\omega - k_{||}v_{||}). \tag{3.3}$$

Setting $s = k_{||}\Delta v_{||}/(k_{||}^2v_\perp^2\bar{\nu})^{1/3}\sim 1$ recovers the earlier estimates and implies

$$\frac{-1}{\mathrm{i}(\omega - k_{||}v_{||})} \sim \bar{\tau}_{\mathrm{int}} = 1/\bar{\nu}_{\mathrm{eff}}\sim\pi\delta(\omega - k_{||}v_{||}), \tag{3.4}$$

thereby providing a physical meaning for the delta function that cannot be obtained by considering a steady state causal Landau resonance. Notice the function

$$\bar{P} = \frac{1}{\pi(k_{||}^2v_\perp^2\bar{\nu})^{1/3}}\int_0^\infty \mathrm{d}t\,\mathrm{e}^{-t^3/3}\cos(st), \tag{3.5}$$

now plays the role of a delta function for $s\gg 1$.

The next section starts to incorporate tokamak geometry.

https://doi.org/10.1017/S002237782400117X Published online by Cambridge University Press

4. Resonant electrons in tokamak geometry without collisions

The preceding section indicates that collisions are very weak, but become significant for the resonant electrons in or near collisional boundary layers. As a result, it is useful to briefly examine the collisionless resonant condition in tokamak geometry, where $\omega - k_{||}v_{||}$ is replaced by its transit-averaged form (Catto & Tolman 2021*a*)

$$\oint_f \mathrm{d}\tau(\omega - k_{||}v_{||}) = \omega\oint_f \mathrm{d}\tau - 2\pi\sigma(qn-m), \tag{4.1}$$

with $\mathrm{d}\tau = \mathrm{d}\vartheta/v_{||}\boldsymbol{n}\cdot\nabla\vartheta \approx qR\,\mathrm{d}\vartheta/v_{||} > 0$ and the subscript f denoting an integration over a full 2π for the passing ($\sigma = v_{||}/|v_{||}| = \pm 1$) and a full bounce for the trapped ($\sigma = 0$).

For a small inverse aspect ratio ($\epsilon \ll 1$) tokamak with

$$B = B_0(1-\epsilon\cos\vartheta), \tag{4.2}$$

and $v_{||}^2 = v^2(1-\lambda B/B_0)$, letting $k^2 = 2\epsilon\lambda/[1-(1-\epsilon)\lambda] = \kappa^{-2}$ leads to

$$\oint_f \mathrm{d}\tau = \frac{4qR}{v\sqrt{2\epsilon}}\begin{cases}\sqrt{(1-\epsilon)k^2+2\epsilon}\,K(k) & \text{passing } (0\le k<1)\\ 2K(\kappa) & \text{trapped } (0\le\kappa<1)\end{cases}, \tag{4.3}$$

with K the complete elliptic integral of the first kind.

No resonance occurs for the trapped electrons. However, for the passing the collisionless resonance condition becomes

$$\frac{|k_{||}|v}{\omega} = \frac{\sqrt{k^2+2\epsilon}\,K(k)}{(\pi/2)\sqrt{2\epsilon}} \rightarrow \begin{cases}\sqrt{k^2+2\epsilon}/\sqrt{2\epsilon} & k^2 \lesssim 2\epsilon\\ \ell n[16/(1-k^2)]/\pi\sqrt{2\epsilon} & k^2\rightarrow 1\end{cases}, \tag{4.4}$$

where $1 \le |k_{||}|v/\omega = |qn-m|v/\omega qR < \infty$, and no passing resonance occurs for $k_{||} = 0$. For lower hybrid and helicon current drive, the freely passing ($k^2 \lesssim 2\epsilon$) are of most interest (Catto & Zhou 2023).

5. Collisional boundary layer in tokamak geometry without poloidal mode coupling

The results of the preceding section are next extended to consider a collisional boundary layer in tokamak geometry when no poloidal mode coupling occurs. In this slightly artificial, but useful to understand, limit the perturbed passing distribution function is periodic in poloidal angle. Using

$$f_1 = f_m\,\mathrm{e}^{\mathrm{i}n\zeta - \mathrm{i}\omega t - \mathrm{i}m\vartheta + \mathrm{i}S(\psi)}, \tag{5.1}$$

and transit averaging, the passing electron kinetic equation (2.5) then yields

$$\mathrm{i}f_m\left[\omega\oint_f\mathrm{d}\tau - 2\pi\sigma(qn-m)\right] + \oint_f\mathrm{d}\tau\, C\{f_m\} = -\oint_f \mathrm{d}\tau\, W_m, \tag{5.2}$$

where

$$\oint_f \mathrm{d}\tau\, C\{f_m\} = \frac{2\nu_e B_0}{x^3}\frac{\partial}{\partial\lambda}\left[\left(\lambda\oint_f\mathrm{d}\tau\frac{\xi^2}{B}\right)\frac{\partial f_m}{\partial\lambda}\right], \tag{5.3}$$

with

$$B_0\oint_f\mathrm{d}\tau\frac{\xi^2}{B} = \frac{4qR\sqrt{2\epsilon}E(k)}{v\sqrt{(1-\epsilon)k^2+2\epsilon}} \rightarrow \frac{4qR}{v}\begin{cases}\pi\sqrt{2\epsilon}/2\sqrt{k^2+2\epsilon} & k^2\lesssim 2\epsilon\\ \sqrt{2\epsilon}/\sqrt{1+\epsilon} & k^2\rightarrow 1\end{cases}, \tag{5.4}$$

and E the complete elliptic integral of the second kind. For a resonant interaction when $qn > m\,(qn < m)$ a passing electron must have $v_{||} > 0\,(v_{||} < 0)$ since $\omega\oint_f \mathrm{d}\tau > 0$.

https://doi.org/10.1017/S002237782400117X Published online by Cambridge University Press

Taylor expanding about the resonant pitch angle λ_{res}

$$\tau_f = \oint_f \mathrm{d}\tau = \tau_f^0 + (\lambda - \lambda_{\text{res}})\partial\tau_f/\partial\lambda|_{\lambda=\lambda_{\text{res}}} + \cdots, \tag{5.5}$$

where $\tau_f^0 = 2\pi|qn - m|/\omega > 0$, gives the Airy form

$$\frac{\partial^2 f_m}{\partial u^2} + \mathrm{i}uf_m \approx -\frac{\oint_f \mathrm{d}\tau\, W_m|_{\lambda=\lambda_{\text{res}}}}{(\nu\tau_f^0)^{1/3}(\omega\partial\tau_f/\partial\lambda|_{\lambda=\lambda_{\text{res}}})^{2/3}}, \tag{5.6}$$

with $\oint_f \mathrm{d}\tau\, W_m \approx \oint_f \mathrm{d}\tau\, W_m|_{\lambda=\lambda_{\text{res}}}$ due to the narrowness of the boundary layer, and

$$u = (\lambda - \lambda_{\text{res}})(\omega\partial\tau_f/\partial\lambda)^{1/3}/(\nu\tau_f^0)^{1/3} = (\lambda - \lambda_{\text{res}})/w. \tag{5.7}$$

In the preceding, the resonance is used to define $k_{\text{res}}^2 = 2\epsilon\lambda_{\text{res}}/[1 - (1-\epsilon)\lambda_{\text{res}}]$ in (4.4) and its narrowness is used to approximate

$$\oint_f \mathrm{d}\tau\, C\{f_m\} \approx \frac{2\nu_e B_0}{x^3}\left(\lambda_{\text{res}}\oint_f \mathrm{d}\tau \left.\frac{\xi^2}{B}\right|_{\text{res}}\right)\frac{\partial^2 f_m}{\partial\lambda^2} \equiv \nu\tau_f^0\frac{\partial^2 f_m}{\partial\lambda^2}, \tag{5.8}$$

with $\nu\tau_f^0 \approx 2\nu_e x^{-3}\lambda_{\text{res}}\oint_f \mathrm{d}\tau\,\xi^2$.

Assuming $k^2 \lesssim 2\epsilon$, then $\lambda \approx k^2/(k^2 + 2\epsilon)$ and $k_0 = k_{\text{res}}$ give

$$\partial\tau_f/\partial\lambda|_{\lambda=\lambda_{\text{res}}} = \pi qR(k_0^2 + 2\epsilon)^{3/2}/v(2\epsilon)^{3/2} \sim qR/v \sim \tau_f^0. \tag{5.9}$$

Then, making use of $\partial/\partial\lambda \sim 1/(\lambda - \lambda_{\text{res}})$ leads to the boundary layer width estimate

$$\lambda - \lambda_{\text{res}} \sim [\nu\tau_f^0/(\omega\partial\tau_f/\partial\lambda|_{\lambda=\lambda_{\text{res}}})]^{1/3} \sim (\nu/\omega)^{1/3}, \tag{5.10}$$

and effective collision frequency estimate

$$\nu_{\text{eff}} \approx \nu/(\lambda - \lambda_{\text{res}})^2 \approx \nu[\omega(\partial\tau_f/\partial\lambda|_{\lambda=\lambda_{\text{res}}})/\nu\tau_f^0]^{2/3} \sim \nu(\omega/\nu)^{2/3}. \tag{5.11}$$

Use of $(\partial^2/\partial u^2 + \mathrm{i}u)\int_0^\infty \mathrm{d}t\, \mathrm{e}^{\mathrm{i}ut - t^3/3} = \int_0^\infty \mathrm{d}t(\partial/\partial t)\, \mathrm{e}^{\mathrm{i}ut - t^3/3} = -1$ leads to the solution

$$f_m^{\text{pass}} = \frac{\oint_f \mathrm{d}\tau\, W_m|_{\lambda=\lambda_{\text{res}}}}{(\omega\partial\tau_f/\partial\lambda|_{\lambda=\lambda_{\text{res}}})w}\int_0^\infty \mathrm{d}t\, \mathrm{e}^{\mathrm{i}ut - t^3/3} \underset{u\to\pm\infty}{\rightarrow} \frac{\mathrm{i}\oint_f \mathrm{d}\tau\, W_m|_{\lambda=\lambda_{\text{res}}}}{\omega\oint_f \mathrm{d}\tau - 2\pi|qn - m|}, \tag{5.12}$$

for the passing, with $w = (\nu\tau_f^0)^{1/3}/(\omega\partial\tau_f/\partial\lambda|_{\lambda=\lambda_{\text{res}}})^{1/3} \sim (\nu/\omega)^{1/3} \ll 1$ in $u = (\lambda - \lambda_{\text{res}})/w$, as expected from $u \approx 1$. In addition, $f_m^{\text{pass}} \propto \nu^{-1/3}$ for $|u| \ll 1$.

https://doi.org/10.1017/S002237782400117X Published online by Cambridge University Press

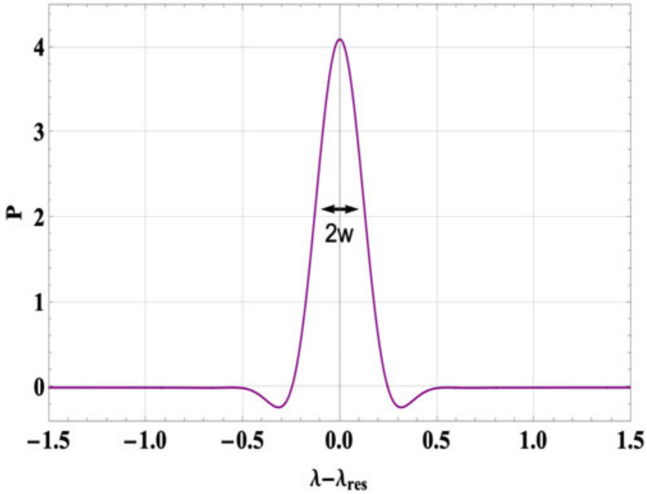

FIGURE 1. A plot of the function P versus pitch angle λ to demonstrate its delta function behaviour in the vicinity of the resonant pitch angle λ_{res} (reprinted with permission from Catto & Tolman 2021*b*).

Integration over velocity space requires an integration over pitch angle ($\mathrm{d}^3 v \approx 2\pi B v^3\,\mathrm{d}v\,\mathrm{d}\lambda / B_0 v_{||}$). In this case

$$P = (\pi w)^{-1} \int_0^\infty \mathrm{d}t\, \mathrm{e}^{-t^3/3} \cos(ut), \tag{5.13}$$

is a delta function representation in pitch angle as shown in figure 1. To see this, let $\varsigma \gg 1$ and recall any integral over velocity space will involve pitch angle, resulting in

$$\int_{\lambda_{res}-\varsigma w}^{\lambda_{res}+\varsigma w} \mathrm{d}\lambda P = \frac{1}{\pi} \int_0^\infty \mathrm{d}t\, \mathrm{e}^{-t^3/3} \int_{-\varsigma}^{\varsigma} \mathrm{d}u \cos(ut) = \frac{2}{\pi} \int_0^\infty \mathrm{d}t\, \mathrm{e}^{-t^3/3} \frac{\sin(\varsigma t)}{t} = 1. \tag{5.14}$$

The function that contains P as its real part will be denoted by

$$U(u) = (\pi w)^{-1} \int_0^\infty \mathrm{d}t\, \mathrm{e}^{\mathrm{i}ut - t^3/3} \underset{u\to\pm\infty}{\to} i/\pi(\lambda - \lambda_{res}). \tag{5.15}$$

Notice that the imaginary part (ImU) is odd in u and dominates asymptotically, while the $P(u) = ReU(u)$ exhibits the delta function behaviour. Therefore

$$\mathrm{Im} \int_{\lambda_{res}-\varsigma w}^{\lambda_{res}+\varsigma w} \mathrm{d}\lambda U = \frac{1}{\pi} \int_0^\infty \mathrm{d}t\, \mathrm{e}^{-t^3/3} \int_{-\varsigma}^{\varsigma} \mathrm{d}u \sin(ut) = 0, \tag{5.16}$$

indicating ImU no longer plays a role once the pitch angle integral is performed

For the trapped electrons ($\sigma = 0$) in (5.2), implying no resonant boundary layers occur and collisions are negligible. As a result, the expected trapped response is

$$f_m^{trap} \approx \mathrm{i}\omega^{-1} \Sigma_m W_m\, \mathrm{e}^{-\mathrm{i}m\vartheta}. \tag{5.17}$$

However, there will be an additional collisional boundary layer about the trapped–passing boundary since both f_m^{trap} and f_m^{pass} must vanish there, as they are different functions of λ. More details will be given in the following sections.

https://doi.org/10.1017/S002237782400117X Published online by Cambridge University Press

Better solutions for the trapped and passing will be given in the subsequent sections when poloidal mode coupling is retained for the trapped as well as the passing alphas. And the trapped–passing boundary layer will also be addressed further in § 8.

6. Poloidal mode coupling with an effective Krook model resolution of singularities

An insightful solution of (2.5) retaining poloidal mode coupling is obtained by making the Krook replacement $C\{f_1\} \to -\nu_{eff} f_1$ with $\nu_{eff} \sim \nu(\omega/\nu)^{2/3}$. Introducing the trajectory time variable τ by letting $\mathrm{d}\tau = \mathrm{d}\vartheta/v_{||}\boldsymbol{n}\cdot\nabla\vartheta > 0$ with $\mathrm{d}\vartheta > 0$ for $v_{||} > 0$, $\mathrm{d}\vartheta < 0$ for $v_{||} < 0$, and $\boldsymbol{n}\cdot\nabla\vartheta > 0$, then integrating from $\tau \to -\infty$ where $f_1 = 0$ to $\tau = 0$ with $\vartheta(\tau = 0) = \vartheta$ gives

$$f_1 = \mathrm{e}^{-\mathrm{i}m\vartheta}\int_{-\infty}^{0} \mathrm{d}\tau\, W_m(\tau)\, \mathrm{e}^{-(\mathrm{i}\omega-\nu_{eff})\tau+\mathrm{i}(qn-m)[\vartheta(\tau)-\vartheta]}. \tag{6.1}$$

To retain trapped and passing electrons f_1 is written in $\psi, \vartheta, \zeta, v, \lambda$ and σ variables. Consequently, successive passes through resonance are strongly correlated, and poloidal variation entering $v_{||}$ by its B dependence is fully retained. Collisional boundary layer modifications are neglected in (6.1). However, they are considered further in subsequent sections once poloidal variation is properly evaluated in (6.2) and (6.3).

The trajectory integral form (6.1) for f_1 is similar to many expressions in the rf literature (Bernstein & Baxter 1981; Belikov & Kolesnichenko 1982, 1994; Brambilla 1989, 1994, 1999; Kasilov *et al.* 1990; Catto & Myra 1992; Lamalle 1993, 1997; Jaeger *et al.* 2001, 2006, 2008; Brambilla & Bilato 2020). The KINETIC-J treatment of Green & Berry (2014) includes a function $\alpha(t')$ under its trajectory integral in their eq. (11) that plays a role similar to a very large ν_{eff}. Taking full advantage of the periodicity of unperturbed orbits and W_m, and defining the time for a full poloidal circuit as $\tau_f = \oint_f \mathrm{d}\vartheta/v_{||}\boldsymbol{n}\cdot\nabla\vartheta > 0$ leads to (Bernstein & Baxter 1981; Belikov & Kolesnichenko 1982; Tolman & Catto 2021)

$$f_1 = \Sigma_m\, \mathrm{e}^{-\mathrm{i}m\vartheta}\frac{\int_{-\tau_f}^{0} \mathrm{d}\tau\, W_m(\tau)\, \mathrm{e}^{-(\mathrm{i}\omega-\nu_{eff})\tau+\mathrm{i}(qn-m)[\vartheta(\tau)-\vartheta]}}{1-\mathrm{e}^{(\mathrm{i}\omega-\nu_{eff})\tau_f-\mathrm{i}2\pi\sigma(qn-m)}}. \tag{6.2}$$

Only for a homogenous magnetic field does the phase factor $\mathrm{i}(\omega - k_{||}v_{||})\tau$ in the exponential vanish at resonance to allow $f_1 \to \mathrm{i}\Sigma_m\, \mathrm{e}^{-\mathrm{i}m\vartheta}W_m/(\omega - k_{||}v_{||})$ in the collisionless limit.

The transit average in the denominator (implied by the appearance of τ_f) indicates successive poloidal circuits are correlated. Each poloidal mode m may couple to other poloidal modes. This behaviour enters through the exponential phase factor in the preceding integral appearing in the numerator and through the denominator. Taylor expanding the denominator by introducing the mode coupling index $\ell = 0, \pm 1, \pm 2, \ldots$ via $1 = \mathrm{e}^{-\mathrm{i}\sigma 2\pi\ell}$, allows each m to couple to neighbouring poloidal modes for each $n \gg 1$

$$f_1 = \mathrm{i}\Sigma_m\, \mathrm{e}^{-\mathrm{i}m\vartheta}\frac{\int_{-\tau_f}^{0} \mathrm{d}\tau\, W_m(\tau)\, \mathrm{e}^{-(\mathrm{i}\omega-\nu_{eff})\tau+\mathrm{i}(qn-m)[\vartheta(\tau)-\vartheta]}}{(\omega+\mathrm{i}\nu_{eff})\tau_f - \mathrm{i}2\pi\sigma(qn-m-\ell)}. \tag{6.3}$$

This type of coupling only matters for the lower $|\ell|$ since for $|\ell| \gg 1$ the rapidly oscillating phase factor in the integral of the numerator reduces the contributions of higher $|\ell|$. Solution (6.3) is valid for trapped and passing electrons. The transit average behaviour of the denominator and drive term alters the spatial and velocity space behaviour of the full wave solution. Inserting the attenuation factor of Lamalle (1993, 1997) decorrelates successive poloidal transits through resonance and removes this poloidal coupling.

https://doi.org/10.1017/S002237782400117X Published online by Cambridge University Press

7. Poloidal mode coupling and collisional boundary layers in tokamak geometry

The Krook solution (6.3) resolves singularities, but does not capture collisional boundary layer physics of the passing electron solution (5.12) for $\ell = 0$, which gives

$$f_1^{\text{pass}} \underset{\ell=0}{\rightarrow} \Sigma_m \frac{\mathrm{e}^{-\mathrm{i}m\vartheta} \int_{-\tau_f}^{0} \mathrm{d}\tau\, W_m \Big|_{\lambda=\lambda_{\text{res}}}}{(\omega \partial \tau_f/\partial \lambda) w} \int_0^\infty \mathrm{d}t\, \mathrm{e}^{\mathrm{i}ut - t^3/3} = \pi \Sigma_m \frac{\mathrm{e}^{-\mathrm{i}m\vartheta} \int_{-\tau_f}^{0} \mathrm{d}\tau\, W_m \Big|_{\lambda=\lambda_{\text{res}}}}{(\omega \partial \tau_f/\partial \lambda)} U(u). \tag{7.1}$$

This form of the solution suggests a satisfactory modification to the Krook model to account for the resonance shift due to the mode coupling index ℓ, is found by letting $qn - m \rightarrow qn - m - \ell$ in (5.2). Then the mode couple shifted resonance occurs at

$$\tau_f^\ell = 2\pi\sigma(qn - m - \ell)/\omega \geq 2\pi qR/v, \tag{7.2}$$

and the expansion about the resonant pitch angle $\lambda_{\text{res}}^\ell$ becomes

$$\tau_f = \oint_f \mathrm{d}\tau = \tau_f^\ell + (\lambda - \lambda_{\text{res}}^\ell) \partial \tau_f/\partial \lambda|_\ell + \cdots . \tag{7.3}$$

Consequently, neglecting the ν_{eff} in the numerator, since collisions are negligible for a single poloidal transit, the linearized passing solution with mode coupling retained might be expected to have close to the following behaviour:

$$f_1^{\text{pass}} \approx \pi \Sigma_{m,\ell} \frac{\mathrm{e}^{-\mathrm{i}m\vartheta} \int_{-\tau_f}^{0} \mathrm{d}\tau\, W_m(\tau)\, \mathrm{e}^{-\mathrm{i}\omega\tau + \mathrm{i}(qn-m)[\vartheta(\tau) - \vartheta]} \Big|_{\lambda=\lambda_{\text{res}}^\ell}}{\omega \partial \tau_f/\partial \lambda|_\ell} U(u_\ell), \tag{7.4}$$

with $U(u_\ell) = (\pi w_\ell)^{-1} \int_0^\infty \mathrm{d}t\, \mathrm{e}^{-t^3/3 - \mathrm{i}u_\ell t}$, $w_\ell = (\nu \tau_f^\ell)^{1/3} / (\omega \partial \tau_f/\partial \lambda|_{\lambda=\lambda_{\text{res}}^\ell})^{1/3}$, $P(u_\ell) = ReU(u_\ell)$ and $u_\ell = (\lambda - \lambda_{\text{res}}^\ell)/w_\ell$.

The pitch angle variation due to k allows additional $\ell \neq 0$ resonances in (7.2). Defining $k_{||}^\ell = (qn - m - \ell)/qR$, the collisionless mode coupled resonances are then at

$$\frac{|k_{||}^\ell| v}{\omega} = \frac{\sqrt{k_\ell^2 + 2\epsilon} K(k_\ell)}{(\pi/2)\sqrt{2\epsilon}} \rightarrow \begin{cases} [(k_\ell^2 + 2\epsilon)/2\epsilon]^{1/2} & k_\ell^2 \lesssim 2\epsilon \\ \ell n[16/(1 - k_\ell^2)]/\pi\sqrt{2\epsilon} & k_\ell^2 \rightarrow 1 \end{cases}, \tag{7.5}$$

where $1 \leq |k_{||}^\ell| v/\omega < \infty$, making $\ell = \ell(k_\ell)$ with

$$k_\ell^2 = 2\epsilon \lambda_{\text{res}}^\ell / [1 - (1 - \epsilon)\lambda_{\text{res}}^\ell]. \tag{7.6}$$

For example, if $\ell(k_0 = 0) = 0$ at $|k_{||}^0| v/\omega = 1$, then there can be other resonances at $\ell(k_\ell \neq 0) \neq 0$. Notice no passing resonances occur for $|k_{||}^\ell| v/\omega \leq 1$.

To clarify the notation, consider an applied rf wave driving a positive current. The rf has to act on the $v_{||} < 0$ passing electrons, requiring $\tau_f^\ell = 2\pi(m - qn + \ell)/\omega > 0$. As a result, for $k_\ell^2 \lesssim 2\epsilon$, $\tau_f^\ell = 4qR(k_\ell^2 + 2\epsilon)^{1/2}/v\sqrt{2\epsilon} \geq \tau_f^0$. Also, $v_{||} < 0$ means $\mathrm{d}\vartheta < 0$ to keep $\mathrm{d}\tau \propto \mathrm{d}\vartheta/v_{||} > 0$, making $\vartheta(\tau) - \vartheta < 0$. Letting $\Theta = \vartheta(\tau)$ to simplify the notation,

https://doi.org/10.1017/S002237782400117X Published online by Cambridge University Press

then $\tau = qR\int_{\vartheta}^{\Theta} \mathrm{d}\vartheta'/v_{||}(\vartheta';\lambda_{\mathrm{res}}^{\ell})$ giving

$$
\begin{aligned}
&\int_{-\tau_f}^{0} \mathrm{d}\tau\, W_m(\tau)\, \mathrm{e}^{-\mathrm{i}\omega\tau+\mathrm{i}(qn-m)[\vartheta(\tau)-\vartheta]}|_{\lambda=\lambda_{\mathrm{res}}^{\ell}} \\
&\quad = -qR\int_{\vartheta}^{\vartheta+2\pi} \mathrm{d}\Theta\, \frac{W_m(\Theta)}{v_{||}(\Theta;\lambda_{\mathrm{res}}^{\ell})}\, \mathrm{e}^{\mathrm{i}\omega qR\int_{\Theta}^{\vartheta}\mathrm{d}\vartheta'/v_{||}(\vartheta';\lambda_{\mathrm{res}}^{\ell})-\mathrm{i}(m-qn)(\vartheta-\Theta)}|_{\lambda=\lambda_{\mathrm{res}}^{\ell}}.
\end{aligned} \tag{7.7}
$$

This form retains poloidal mode coupling, which occurs since $v_{||}$ cannot be constant in a tokamak so the phase factor under the integral cannot vanish as it does for a uniform magnetic field. It uses the resonance condition to write $v_{||}^2(\Theta;\lambda_{\mathrm{res}}^{\ell}) = v^2[1-\lambda_{\mathrm{res}}^{\ell}B(\Theta)/B_0]$. A $v_{||}<0$ electron starts from $\vartheta+2\pi$ and moves to ϑ in the time τ_f for a passing poloidal circuit.

The solution (6.3) is also valid for the trapped electrons when τ_f is the time for a full bounce and $\sigma = 0$. When the integration in denominator is also over a full bounce

$$
f_1^{\mathrm{trap}} = \Sigma_m\, \mathrm{e}^{-\mathrm{i}m\vartheta}\, \frac{\int_{-\tau_f}^{0}\mathrm{d}\tau\, W_m(\tau)\, \mathrm{e}^{-(\mathrm{i}\omega-\nu_{\mathrm{eff}})\tau+\mathrm{i}(qn-m)[\vartheta(\tau)-\vartheta]}}{1-\mathrm{e}^{(\mathrm{i}\omega-\nu_{\mathrm{eff}})\tau_f}}. \tag{7.8}
$$

Recalling the trapped form of τ_f and using $1=\mathrm{e}^{\mathrm{i}2\pi\ell}$, a collisionless resonance requires

$$
\omega\tau_f = \frac{8\omega qR}{v\sqrt{2\epsilon}}K(\kappa) = 2\pi\ell \geq \frac{4\pi\omega qR}{v\sqrt{2\epsilon}}. \tag{7.9}
$$

The high frequency limit is made tractable by assuming $\omega\tau_f/2\pi = \ell \gg 1$. Then integration by parts and the periodicity of the trapped motion over a full bounce leads to

$$
f_1^{\mathrm{trap}} \approx \mathrm{i}\Sigma_m\, \mathrm{e}^{-\mathrm{i}m\vartheta} W_m/\omega + \cdots . \tag{7.10}
$$

The same result is obtained by solving the high-frequency limit of (2.5).

In the low frequency limit $\omega\tau_f/2\pi \ll 1$ there is no resonance and the trapped response remains small since

$$
f_1^{\mathrm{trap}} \approx \frac{\mathrm{i}qR\mathrm{e}^{-\mathrm{i}qn\vartheta}}{\omega\tau_f}\Sigma_m \oint \mathrm{d}\Theta\, W_m(\Theta)\, \mathrm{e}^{\mathrm{i}(qn-m)\Theta}/v_{||}(\Theta) \underset{|qn-m|\gg 1}{\rightarrow} 0. \tag{7.11}
$$

Consequently, only for low ($\ell \sim 1$) mode coupling indices can the trapped have a significant response. To simplify the presentation in subsequent sections, $f_1^{\mathrm{trap}} \approx 0$ is assumed from here on. The analysis in the next section adds further support to this assumption.

8. The effect of the collisional boundary layer at the trapped–passing boundary

It is not possible to obtain a rigorous analytic solution retaining pitch angle scattering collisions as well as poloidal mode coupling associated with the mode coupling index ℓ of (6.3). In fact, even the approximate passing solution already presented in § 7 is incomplete. It does not account for the trapped–passing boundary where f_1^{pass} must vanish.

In this section, the passing solution is reconsidered for a resonance near the trapped–passing boundary where $\tau_f \propto K(k) \propto -\ell n(1-k^2)$ causes the Taylor expansion to fail since $\partial\tau_f/\partial\lambda \rightarrow 1/[2\epsilon(1-k^2)]$. Recall from § 4 that the collisionless resonance

https://doi.org/10.1017/S002237782400117X Published online by Cambridge University Press

condition for the barely passing electrons ($k^2 \to 1$) in the absence of poloidal mode coupling is

$$\frac{|k_{||}|v}{\omega} = \frac{|qn-m|v}{\omega qR} \approx -\frac{\ell n(1-k^2)}{\pi\sqrt{2\epsilon}}, \tag{8.1}$$

since $\oint_f \mathrm{d}\tau \approx -(2qR/v\sqrt{2\epsilon})\ell n(1-k^2)$. The trapped–passing boundary layer requires very large $|k_{||}|$ at resonance (a large $|k_{||}|$ upshift) due to resonant m being very different in trapped–passing boundary layer than in the more freely passing boundary layers.

Using $2\epsilon\, \mathrm{d}k^2 \approx \mathrm{d}\lambda$, the barely passing limit of the collision operator becomes

$$\oint_f \mathrm{d}\tau C \approx \frac{8qR\nu_e}{(2\epsilon)^{3/2}vx^3}\frac{\partial^2 f_m}{\partial(k^2)^2}. \tag{8.2}$$

Therefore, the boundary layer limit of (5.1)–(5.4) yields

$$-\mathrm{i}[(2\omega qR/v\sqrt{2\epsilon})\ell n(1-k^2) + 2\pi\sigma(qn-m)]f_m + \frac{8qR\nu_e}{(2\epsilon)^{3/2}vx^3}\frac{\partial^2 f_m}{\partial(k^2)^2} \approx -\oint_f \mathrm{d}\tau W_m, \tag{8.3}$$

with $\sigma(qn-m) > 0$ required for a passing resonance. Letting

$$\gamma = e^{\Pi}, \tag{8.4}$$

with

$$\Pi = \frac{\pi\sqrt{2\epsilon}\sigma(qn-m)v}{\omega qR} \gtrsim 1, \tag{8.5}$$

the preceding boundary layer equation becomes

$$\frac{2\nu_e}{\epsilon\omega x^3}\frac{\partial^2 f_m}{\partial(k^2)^2} - \mathrm{i}\ell n[\gamma(1-k^2)]f_m = -\frac{v\sqrt{2\epsilon}}{2\omega qR}\oint_f \mathrm{d}\tau W_m. \tag{8.6}$$

This form of the kinetic equation allows two types of collisional responses. The first response is the one already considered. It is sometimes referred to as a resonant plateau response, indicating it will give a result independent of collision frequency upon integration over pitch angle (as in the plateau regime of neoclassical theory). The second response is collisionally dependent and proportional to $\sqrt{\nu_e}$. To verify this behaviour analytically, $\gamma \gg 1$ must be assumed. Then $y = \gamma(1-k^2)$ can be expanded about $y = 1$ while keeping $k^2 \approx 1$. Keeping only $\ell n(y) \approx y - 1$, and letting $z = (y-1)/\delta$, with

$$\delta = \gamma^{2/3}x^{-1}(2\nu_e/\epsilon\omega)^{1/3} \ll 1, \tag{8.7}$$

then

$$\frac{\partial^2 f_m}{\partial z^2} - \mathrm{i}zf_m = -\frac{v\sqrt{2\epsilon}}{2\omega qR\delta}\oint_f \mathrm{d}\tau W_m. \tag{8.8}$$

To solve, define

$$f_m = \left(\frac{v\sqrt{2\epsilon}}{2\omega qR\delta}\oint_f \mathrm{d}\tau W_m\right)\Upsilon(z), \tag{8.9}$$

https://doi.org/10.1017/S002237782400117X Published online by Cambridge University Press

where $\Upsilon(z)$ is the desired solution to the more familiar inhomogeneous Airy equation

$$\partial^2\Upsilon/\partial z^2 - \mathrm{i}z\Upsilon = -1. \tag{8.10}$$

In the absence of a trapped–passing boundary condition needing to be satisfied, the solution is as before, namely the nearly freely passing resonant plateau (rp) solution

$$\Upsilon_{rp} = \int_0^{\infty} \mathrm{d}\tau\, \mathrm{e}^{-\mathrm{i}z\tau-\tau^3/3} \underset{|z|\gg 1}{\rightarrow} \frac{-\mathrm{i}}{z} = \frac{-\mathrm{i}\delta}{y-1}. \tag{8.11}$$

To make Υ vanish at the trapped–passing boundary $z = -1/\delta$, as well as at $|z| \gg 1$, a homogeneous solution is required. Proceeding as in Catto, Tolman & Parra (2023), but for the passing rather than the trapped, gives the desired solution

$$\Upsilon = \Upsilon_{rp}(z) - \Upsilon_{rp}(z=-1/\delta)Ai(z\,\mathrm{e}^{\mathrm{i}\pi/6})/Ai(-\mathrm{e}^{\mathrm{i}\pi/6}/\delta) \equiv \Upsilon_{rp}(z) + \Upsilon_{\sqrt{\nu}}(z), \tag{8.12}$$

where the Ai are Airy functions (Abramowitz & Stegun 1964). The $\Upsilon_{\sqrt{\nu}}(z)$ contribution arises from the need to make the passing response vanish at the trapped–passing boundary.

When Υ is integrated over pitch angle, or more conveniently z, and exponentially small terms are ignored because $\delta \ll 1$, then

$$Re\int_{-1/\delta}^{(y-1)/\delta} \mathrm{d}z\Upsilon_{\sqrt{\nu}}(z) \approx \frac{\delta^{3/2}}{2^{1/2}}, \tag{8.13}$$

with $\delta^{3/2} = y(2\nu_e/\epsilon\omega x^3)^{1/2}$ and $x^3 > 1$ (due to the high-speed expansion of C), and

$$Re\int_{-1/\delta}^{(y-1)/\delta} \mathrm{d}z\Upsilon(z) = \pi\left(1 + \frac{\delta^{3/2}}{2^{1/2}\pi}\right). \tag{8.14}$$

As a result, the $\sqrt{\nu_e}$ term from the trapped–passing boundary condition is expected to give a small contribution in the core. The trapped are expected to give similar $\sqrt{\nu_e}$. However, at the edge of a tokamak, larger $\delta \sim 1$ may occur so the analysis here may need to be extended. In the earlier sections, the $\sqrt{\nu_e}$ contribution has been treated as negligible by assuming $\delta \ll 1$.

The preceding sections suggest the KINETIC-J code (Green & Berry 2014) can be improved by using (6.3) as the solution, along with the passing particle replacement

$$\frac{\mathrm{i}}{(\omega + \mathrm{i}\nu_{\mathrm{eff}})\tau_f - \mathrm{i}2\pi\sigma(qn - m - \ell)} \rightarrow \frac{1}{\pi w^{\ell}_{\mathrm{res}}}\int_0^{\infty} \mathrm{d}t\, \mathrm{e}^{\mathrm{i}u_\ell t - t^3/3}, \tag{8.15}$$

to remove any undesirable singular behaviour. Here, $u_\ell = [\omega\tau_f - \mathrm{i}2\pi\sigma(qn - m - \ell)]/w^{\ell}_{\mathrm{res}}$ with $w^{\ell}_{\mathrm{res}} \equiv w_\ell\omega\partial\tau_f/\partial\lambda|_{\lambda=\lambda^{\ell}_{\mathrm{res}}}$ except very near the trapped–passing boundary.

9. Comments on electron (and ion) cyclotron heated plasmas

The material in the preceding sections focuses on the lower hybrid and helicon wave regimes for simplicity. However, cyclotron resonances are only slightly more involved for the electrons. For the ions similar treatments are also valid, although finite drift departures from flux surfaces may add complications. In this section, only a simple electron cyclotron resonance is considered as an illustration.

https://doi.org/10.1017/S002237782400117X Published online by Cambridge University Press

To simplify the treatment further, effects associated with the trapped–passing boundary condition are ignored and large aspect ratio is assumed. Moreover, on axis heating is assumed by letting $\omega = \Omega_0 = eB_0/mc$ to write

$$\Omega = \Omega_0(1 - \epsilon \cos\vartheta) = \omega(1 - \epsilon\cos\vartheta). \tag{9.1}$$

Then the collisionless resonance conditions for the passing and trapped electrons from

$$\oint_f \mathrm{d}\tau\,(\omega - \Omega - k_{||}v_{||}) = \oint_f \mathrm{d}\tau\,(\epsilon\omega\cos\vartheta - k_{||}v_{||}) = 0, \tag{9.2}$$

are

$$2\pi\sigma(qn - m) = \epsilon\omega\oint_f \mathrm{d}\tau\cos\vartheta = \frac{4\epsilon\omega qR}{v\sqrt{2\epsilon}}\begin{cases} k^{-2}\sqrt{(k^2+2\epsilon)}[2E(k) - (2-k^2)K(k)] & \text{passing} \\ 2[2E(\kappa) - K(\kappa)] & \text{trapped} \end{cases}. \tag{9.3}$$

The passing condition for a resonance is slightly more involved than before, but once again Taylor expansions about the resonant λ or k can be employed to find behaviour similar to what has already been discussed.

At first glance it might appear there is not a resonance for the trapped, however, $2E(\kappa) = K(\kappa)$ at $\kappa = 0.91$ to give resonant plateau behaviour (Tolman & Catto 2021). Consequently, the trapped are heated, but they are unable to drive current as $v_{||}$ does not enter. Poloidal mode coupling will occur for the trapped as well as the passing as before.

Similar behaviour will occur for ion cyclotron heated ions, with magnetic drifts included in the resonance to retain finite drift departures off flux surfaces. The transit averaging of the wave–particle resonances may alter some of the velocity space structure observed in AORSA simulations (Jaeger *et al.* 2006, 2008).

10. Improved quasilinear operators

The general expression for the rf quasilinear operator retaining the full transit averaged correlated resonance condition and including poloidal mode coupling was derived by Catto & Tolman (2021*a*) in the resonant plateau limit and is given by their (7.11)–(7.13). It leads to the correct entropy production as shown by their (7.14). In the lower hybrid and helicon limit considered here, for a single applied wave frequency and toroidal mode number, their quasilinear operator acting on a Maxwellian f_0 has the form

$$Q\{f_0\} = \Sigma_{m,S}\frac{1}{v\tau_f}\frac{\partial}{\partial v}\left(v\tau_f D\frac{\partial f_0}{\partial v}\right), \tag{10.1}$$

with the quasilinear diffusivity D given by

$$D = \frac{\pi e^2}{2m^2v^2\tau_f}\Sigma_\ell\,\delta\left(\oint_f \mathrm{d}\tau\,\Lambda - 2\pi\sigma\ell\right)\left|J_0(\eta)\boldsymbol{e}_m\cdot\boldsymbol{n}\int_{-\tau_f}^{0}\mathrm{d}\tau\,v_{||}\,\mathrm{e}^{-\mathrm{i}\omega\tau + \mathrm{i}(qn-m)[\vartheta(\tau)-\vartheta]}\right.$$
$$\left. + \mathrm{i}J_1(\eta)\frac{\lambda^{1/2}}{k_\perp}\boldsymbol{e}_m\cdot\boldsymbol{k}\times\boldsymbol{n}\int_{-\tau_f}^{0}\mathrm{d}\tau\,v\,\mathrm{e}^{-\mathrm{i}\omega\tau + \mathrm{i}(qn-m)[\vartheta(\tau)-\vartheta]}\right|^2, \tag{10.2}$$

for $v_\perp \approx \lambda^{1/2}v$ and $\eta \approx k_\perp\lambda^{1/2}v/\Omega_0$. The subscripts on the sums indicate poloidal (m) and radial (S) modes are to be summed over, and for each m, the ℓ modes it couples to must also be summed over. In addition, $\oint_f \mathrm{d}\tau\,\Lambda = \omega\tau_f - 2\pi\sigma(qn - m)$, and the trapped

https://doi.org/10.1017/S002237782400117X Published online by Cambridge University Press

electron response has been assumed negligible based on the estimates of § 7. If the lowest electron cyclotron resonance is retained then $\oint_f \mathrm{d}\tau\,\Lambda = \oint_f \mathrm{d}\tau(\omega - \Omega) - 2\pi\sigma(qn - m)$, and the term inside $|\cdots|^2$ needs to be generalized as found by Catto & Tolman (2021*a*).

The singular behaviour of the delta function can be removed by the replacement

$$\delta\left(\oint_f \mathrm{d}\tau\,\Lambda - 2\pi\ell\right) \to \frac{\int_0^\infty \mathrm{d}t\,\mathrm{e}^{-t^3/3}\cos(u_\ell t)}{\pi w_\ell \partial(\oint_f \mathrm{d}\tau\,\Lambda)/\partial\lambda|_{\lambda=\lambda_{\mathrm{res}}^\ell}}, \tag{10.3}$$

with

$$P(u_\ell) = (\pi w_\ell)^{-1}\int_0^\infty \mathrm{d}t\,\mathrm{e}^{-t^3/3}\cos(u_\ell t), \tag{10.4}$$

acting as a delta function when integrated over pitch angle. Here, $u_\ell = (\lambda - \lambda_{\mathrm{res}}^\ell)/w_\ell$ and $w_\ell = (\nu\tau_f^\ell)^{1/3}/[\partial(\oint_f \mathrm{d}\tau\,\Lambda)/\partial\lambda_{\lambda=\lambda_{\mathrm{res}}^\ell}]^{1/3}$. For each ℓ the preceding expressions give

$$\int \mathrm{d}\lambda\delta\left(\oint_f \mathrm{d}\tau\,\Lambda - 2\pi\ell\right) \to 1/\partial\left(\oint_f \mathrm{d}\tau\,\Lambda\right)/\partial\lambda|_{\lambda=\lambda_{\mathrm{res}}^\ell}, \tag{10.5}$$

as $\int \mathrm{d}\lambda P(u_\ell) \to 1$ when integrated over λ region about $\lambda_{\mathrm{res}}^\ell$ a few w_ℓ wide. The replacement (10.3) is valid away from the trapped–passing boundary. This substitution improves on the one suggested in Tolman & Catto (2021) by more precisely accounting for tokamak geometry. In the vicinity of the trapped–passing boundary the resonant plateau response Υ_{rp} has to be replaced by the full response $\Upsilon_{rp} + \Upsilon_{\sqrt{\nu}}$, as discussed in § 6.

11. Improved linear response to include poloidal mode coupling

Evaluating the perturbed density and current in tokamak geometry is complicated by the presence of the τ or Θ integral associated with the trajectory integration over the near periodic motion in (7.4). However, some simplification is possible since the trapped are expected to be unimportant and only $\mathrm{Im}U(u_\ell) = P(u_\ell)$ survives the λ integration over $\mathrm{d}^3v \to Bv^2\,\mathrm{d}v\,\mathrm{d}\lambda\,\mathrm{d}\varphi/B_0\sqrt{1-\lambda B/B_0}$. Moreover, since $P(u_\ell)$ behaves as a delta function to lowest order the replacement $P(u_\ell) \to \delta(\lambda - \lambda_{\mathrm{res}}^\ell)$ can be employed. For example, using (7.4), the perturbed charge density and parallel current are given by

$$e\int_{\mathrm{pass}} \mathrm{d}^3v\,v_{||}^j f_1^{\mathrm{pass}} \approx \pi e\Sigma_{m,\ell}\,\mathrm{e}^{-\mathrm{i}m\vartheta}\int_{\mathrm{pass}} \mathrm{d}^3v\,v_{||}^j \frac{\delta(\lambda-\lambda_{\mathrm{res}}^\ell)}{\omega\partial\tau_f/\partial\lambda|_\ell}\int_{-\tau_f}^0 \mathrm{d}\tau\,W_m(\tau)\,\mathrm{e}^{-\mathrm{i}\omega\tau+\mathrm{i}(qn-m)[\vartheta(\tau)-\vartheta]}, \tag{11.1}$$

with $j=0$ or 1 and where, by approximating $v_\perp \approx \lambda^{1/2}v$ and $\eta \approx k_\perp\lambda^{1/2}v/\Omega_0$, their poloidal angle dependence can be ignored. In addition, the gyrophase integral can be performed to recover another Bessel function from the $\mathrm{e}^{-\mathrm{i}L}$ factor in W_m to find

$$\begin{aligned} e\int_{\mathrm{pass}} \mathrm{d}^3v\,v_{||}^j f_1^{\mathrm{pass}} \approx &-\frac{\pi e^2}{T}\Sigma_{m,\ell}\,\mathrm{e}^{-\mathrm{i}m\vartheta}\int_{\mathrm{pass}} \mathrm{d}^3v\,v_{||}^j f_0 \frac{\delta(\lambda-\lambda_{\mathrm{res}}^\ell)}{\omega\partial\tau_f/\partial\lambda|_\ell} J_0(\eta)\{J_0(\eta)\boldsymbol{e}_m\cdot\boldsymbol{n} \\ &\int_{-\tau_f}^0 \mathrm{d}\tau\,v_{||}\,\mathrm{e}^{-\mathrm{i}\omega\tau+\mathrm{i}(qn-m)[\vartheta(\tau)-\vartheta]} + \mathrm{i}J_1(\eta)\frac{\lambda^{1/2}}{k_\perp}\boldsymbol{e}_m\cdot\boldsymbol{k}\times\boldsymbol{n}\int_{-\tau_f}^0 \mathrm{d}\tau\,v\,\mathrm{e}^{-\mathrm{i}\omega\tau+\mathrm{i}(qn-m)[\vartheta(\tau)-\vartheta]}\Bigg\}. \end{aligned} \tag{11.2}$$

Due to the presence of the delta function, only a speed integral over v and the trajectory integral over a period need be performed, as $\int \mathrm{d}\varphi = 2\pi$. The speed integral could be performed in the usual manner to obtain a modified Bessel function form if it were not for the exponential coupling factor. Its existence highlights the need to sum over all the poloidally coupled modes as indicated by the ℓ sum for each m summed. A similar expression holds for the perpendicular flow, but with the overall $J_0(\eta)$ multiplier in front of $\{\cdots\}$ in the $j=0$ form of (11.2) replaced by $\mathrm{i}v_\perp k_\perp^{-1} J_1(\eta)\boldsymbol{k}\times\boldsymbol{n}$.

Once the replacement $P(u_\ell)\rightarrow\delta(\lambda-\lambda_{res}^{\ell})$ is made, the collision frequency no longer appears. Its absence does not mean rf quasilinear theory is collisionless. Instead, the absence of the collision frequency is a signature of the resonant plateau behaviour of the boundary layers associated with the wave–particle resonance. Fortunately, the details of the boundary layers about the trapped–passing boundary seem to be relatively unimportant as long as (8.7) is satisfied.

12. Limitations of a quasilinear treatment

It is possible to make some simple estimates of when quasilinear treatments of rf might fail (Catto 2020; Catto & Tolman 2021*a*,*b*). To begin, notice that the quasilinear operator will compete with the collision operator to make f_0 depart from Maxwellian when

$$Q\{f_0\}/C\{f_0\}\sim D/v_e^2\nu\sim 1. \tag{12.1}$$

Recalling from (5.11) that $\nu_{\mathrm{eff}}\sim\nu(\omega/\nu)^{2/3}$, $\delta(\oint_f \mathrm{d}\tau\,\varLambda-2\pi\ell)\sim\omega/\nu_{\mathrm{eff}}\sim(\omega/\nu)^{1/3}$ giving

$$D\sim(e|\boldsymbol{e}_m|/m)^2\,\delta\left(\oint_f \mathrm{d}\tau\,\varLambda-2\pi\ell\right)/\omega\sim(e|\boldsymbol{e}_m|/m)^2/\nu_{\mathrm{eff}}. \tag{12.2}$$

Therefore, substantial distortion is expected when

$$e|\boldsymbol{e}_m|/mv_e\sim\nu(\omega/\nu)^{1/3}. \tag{12.3}$$

Quasilinear theory assumes

$$1\gg\frac{|\nabla_v f_1|}{|\nabla_v f_0|}\sim\frac{f_1/wv_e}{f_0/v_e}, \tag{12.4}$$

where $w\sim(\nu/\omega)^{1/3}\ll 1$ from § 5. Therefore, it requires

$$f_1/f_0\ll(\nu/\omega)^{1/3}. \tag{12.5}$$

However, from § 7

$$f_1\sim\frac{W_m}{\omega}\delta(\lambda-\lambda_{res})\sim\frac{e|\boldsymbol{e}_m|f_0}{mv_e\omega w}, \tag{12.6}$$

requiring

$$e|\boldsymbol{e}_m|/mv_e\ll\nu(\omega/\nu)^{1/3}, \tag{12.7}$$

and, thereby, a negligible distortion of the Maxwellian according to (12.1).

These estimates suggest that quasilinear theory is failing once the unperturbed distribution function becomes significantly distorted from Maxwellian (as it does in most non-adjoint treatments of rf). When this happens the nonlinear term needs to be retained in the perturbed kinetic equation to account for island formation.

13. Discussion

The preceding sections attempt to outline a more comprehensive and, in some ways, unconventional view of the linear solution used for rf quasilinear theory in a tokamak. The earlier sections establish the importance of collisional boundary layers, while later sections demonstrate that collisions cancel out of the final expressions for the perturbed density and current to lowest order, as shown in detail in § 11, by (11.2). The disappearance of the collision frequency is not an indication that collisions do not matter, but rather is a signature of the resonant plateau behaviour inherent in using unperturbed trajectories to treat wave–particle resonances in a linearized kinetic equation (Catto & Tolman 2021*b*). Such behaviour occurs when a diffusive collision operator resolves the singularity that arises from a velocity dependent wave–particle resonance. Collisions also enter explicitly from the collisional boundary layers about the trapped–passing boundary, but these contributions are expected to be small, and (6.3) with the replacement (8.15) is expected to be an adequate solution

$$f_1 = \mathrm{i}\Sigma_{m,\ell}\frac{\mathrm{e}^{-\mathrm{i}m\vartheta}}{\pi w^{\ell}_{\mathrm{res}}}\int_0^\infty \mathrm{d}t\,\mathrm{e}^{\mathrm{i}u_\ell t-t^3/3}\int_{-\tau_f}^{0}\mathrm{d}\tau\,W_m(\tau)\,\mathrm{e}^{-\mathrm{i}\omega\tau+\mathrm{i}(qn-m)[\vartheta(\tau)-\vartheta]}. \tag{13.1}$$

The treatment here attempts to do justice to tokamak geometry when solving the linearized kinetic equation. The various solution techniques considered illustrate that poloidal mode coupling (as retained by the index ℓ) must be retained since the parallel velocity depends sensitively on the poloidal variation of the magnetic field and is of course responsible for the presence of trapped as well as passing particles. These details are typically neglected in the rf treatments of the linearized physics because mirror force effects are mistreated. The variation of the parallel velocity with poloidal angle allows each poloidal mode to couple with many other poloidal modes. The Krook model solution, (6.3), presented in § 6, is shown to retain this coupling while ignoring boundary layers. Next, an approximate extension to a diffusive collision operator is suggested in § 7, by (7.4). It seems to sensibly treat the collisional boundary layers for the various wave–particle resonances. As only lowest-order collisional results are needed, as shown, it provides what seems to be a serviceable and physical representation for a delta function.

The techniques developed here are also applicable for wave frequencies comparable to the cyclotron frequency as briefly discussed in § 9, and shown by (9.3). Notably, the wave–particle resonances that appear in the transit average form of the linearized solution of the kinetic equation are consistent with a proper quasilinear treatment (Catto & Tolman 2021*a*). The form implies that the resonance is transit averaged and not localized. The resonant interaction time $\tau_{\mathrm{int}} = 1/\nu_{\mathrm{eff}}$ is long compared with the time to complete many poloidal circuits. Hence, assuming uncorrelated kicks at the local resonance is incorrect. Any actual spatial localization likely has more to do with the spatial behaviour of the applied rf drive term on the right side of the kinetic equation.

Finally, some simple estimates, (12.3) and (12.7), are given in § 12 to show that, once the applied rf amplitude is strong enough for the quasilinear operator, (10.1) and (10.2), described in § 10 to distort the unperturbed distribution function significantly from Maxwellian, the quasilinear approach is failing because the linearized solution to the kinetic equation is no longer valid. If these estimates are correct, then there is no need to evolve distribution functions to treat non-Maxwellian features when performing quasilinear heating and current drive evaluations. Said another way, once a distortion of the unperturbed Maxwellian occurs, a linearized solution of the kinetic equation is no longer valid.

https://doi.org/10.1017/S002237782400117X Published online by Cambridge University Press

The unconventional procedures presented here for solving the linearized kinetic equation, that is the basis for rf quasilinear theory, include the retention of the collisional boundary layers enclosing and broadening wave–particle resonances (making rf quasilinear theory collisional – rather than collisionless – as required for consistency), the occurrence of transit averaged (rather than spatially local) resonances, the presence of collisional boundary layers at the trapped–passing boundary, the treatment of tokamak geometry leading to the coupling of poloidal modes via the index ℓ in (13.1), and the anticipated failure of rf quasilinear theory once the unperturbed distribution function distorts from Maxwellian. Perhaps the insights outlined here to highlight these physical effects will improve the success rf simulations have achieved, lead to an appreciation of their explicit geometric and implicit collisional natures, and further improve simulations.

Acknowledgements

The author is grateful to P. Bonoli for motivation, support and patient discussions, and to J. Wright for his many helpful suggestions that have clarified the presentation and his generous help with references. The United States Government retains a non-exclusive, paid-up, irrevocable, worldwide license to publish or reproduce the published form of this manuscript, or allow others to do so, for United States Government purposes.

Editor Per Helander thanks the referees for their advice in evaluating this paper.

Funding

This work was supported by the U.S. Department of Energy under contract number DE-FG02-91ER-54109.

Declaration of interests

The author reports no conflict of interest.

REFERENCES

ABRAMOWITZ, M. & STEGUN, I.A. 1964 *Handbook of Mathematical Functions with Formulas, Graphs, and Mathematical Tables*, 10th printing, pp. 446–449. National Bureau of Standards.

BELIKOV, V.S. & KOLESNICHENKO, Y.I. 1982 Derivation of the quasi-linear theory equations for the axisymmetric toroidal systems. *Plasma Phys*. **24**, 61–72.

BELIKOV, V.S. & KOLESNICHENKO, Y.I. 1994 Quasilinear theory for a tokamak plasma in the presence of cyclotron resonance. *Plasma Phys. Control. Fusion* **36**, 1703–1718.

BERNSTEIN, I.B. & BAXTER, D.C. 1981 Relativistic theory of electron cyclotron resonance heating. *Phys. Fluids* **24**, 108–126.

BONOLI, P.T. 2014 Review of recent experimental and modeling progress in the lower hybrid range of frequencies at ITER relevant parameters. *Phys. Plasmas* **21**, 061508.

BRAMBILLA, M. 1989 Finite Larmor radius wave equations in tokamak plasmas in the ion cyclotron frequency range. *Plasma Phys. Control. Fusion* **31**, 723–757.

BRAMBILLA, M. 1994 A note on the toroidal plasma dispersion relation. *Phys. Lett.* A **188**, 376–383.

BRAMBILLA, M. 1999 Numerical simulation of ion cyclotron waves in tokamak plasmas. *Plasma Phys. Control. Fusion* **41**, 1–34.

BRAMBILLA, M. & BILATO, R. 2020 Toroidicity effects on the absorption of IC waves by electrons. *Nucl. Fusion* **60**, 096016.

CATTO, P.J. 1978 Linearized gyrokinetics. *Plasma Phys.* **20**, 719–722.

CATTO, P.J. 2019 Practical gyrokinetics. *J. Plasma Phys.* **85**, 925850301.

CATTO, P.J. 2020 Collisional effects on resonant particles in quasilinear theory. *J. Plasma Phys*. **86**, 815860302.

CATTO, P.J. 2021 Lower hybrid current drive in a tokamak for correlated passes through resonance. *J. Plasma Phys*. **87**, 905870309.

CATTO, P.J. & MYRA, J.R. 1992 A quasilinear description for fast-wave minority heating permitting off-magnetic axis heating in a tokamak. *Phys. Fluids* B **4**, 187–199.

CATTO, P.J. & TOLMAN, E.A. 2021*a* Reimagining full wave quasilinear theory in a tokamak. *J. Plasma Phys*. **87**, 905870215.

CATTO, P.J. & TOLMAN, E.A. 2021*b* Collisional broadening of nonlinear resonant wave-particle interactions. *J. Plasma Phys*. **87**, 905870606.

CATTO, P.J., TOLMAN, E.A. & PARRA, F.I. 2023 Merging of the super banana plateau and transport regimes in nearly quasisymmetric stellarators. *J. Plasma Phys*. **89**, 905890106.

CATTO, P.J. & ZHOU, M. 2023 Helicon and lower hybrid current drive comparisons in tokamak geometry. *J. Plasma Phys*. **89**, 905890405.

GREEN, D.L. & BERRY, L.A. 2014 Iterative addition of parallel temperature effects to finite difference simulation of radio-frequency wave propagation in plasmas. *Comput. Phys. Commun*. **185**, 736–743.

JAEGER, E.F., BERRY, L.A., D'AZEVEDO, E., BARRET, R.F., AHERN, S.D., SWAIN, D.W., BATCHELOR, D.B., HARVEY, R.W., MYRA, J.R., D'IPPOLITO, D.A., PHILLIPS, C.K., VALEO, E., SMITHE, D.N., BONOLI, P.T., WRIGHT, J.C. & CHOI, M. 2008 Simulation of high-power electromagnetic wave heating in the ITER burning plasma. *Phys. Plasmas* **15**, 072513.

JAEGER, E.F., BERRY, L.A., D'AZEVEDO, E., BATCHELOR, D.B. & CARTER, M.D. 2001 All-orders spectral calculation of radio-frequency heating in two-dimensional toroidal plasmas. *Phys. Plasmas* **8**, 1573–1583.

JAEGER, E.F., HARVEY, R.W., BERRY, L.A., MYRA, J.R., DUMONT, R.J., PHILLIPS, C.K., SMITHE, D.N., BARRET, R.F., BATCHELOR, D.B., BONOLI, P.T., CARTER, M.D., D'AZEVEDO, E.F., D'IPPOLITO, D.A., MOORE, R.D. & WRIGHT, J.C. 2006 Global-wave solutions with self-consistent velocity distributions in ion cyclotron heated plasmas. *Nucl. Fusion* **46**, S397–S408.

KASILOV, S.V., PYATAK, A.I. & STEPANOV, K.N. 1990 Cyclotron resonance for fast magnetosonic waves in inhomogeneous magnetic fields of toroidal confinement devices. *Nucl. Fusion* **30**, 2467–2495.

KENNEL, C.F. & ENGELMANN, F. 1966 Velocity space diffusion from weak plasma turbulence in a magnetic field. *Phys. Fluids* **9**, 2377–2388.

LAMALLE, P.U. 1993 The nonlocal radio-frequency response of a toroidal plasma. *Phys. Lett.* A **175**, 45–52.

LAMALLE, P.U. 1997 On the radiofrequency response of tokamak plasmas. *Plasma Phys. Control. Fusion* **39**, 1409–1460.

LEE, J.-P., SMITHE, D., WRIGHT, J. & BONOLI, P. 2018 A positive-definite form of bounce-averaged quasilinear velocity diffusion for the parallel inhomogeneity in a tokamak. *Plasma Phys. Control. Fusion* **60**, 025007.

MENEGHINI, O., SHIRAIWA, S. & PARKER, R. 2009 Full wave simulation of lower hybrid waves in Maxwellian plasma based on the finite element method. *Phys. Plasmas* **16**, 090701.

PETROV, Y.V. & HARVEY, R.W. 2016 A fully-neoclassical finite-orbit-width version of the CQL3D Fokker-Planck code. *Plasma Phys. Control. Fusion* **58**, 115001.

PRATER, R., MOELLER, C.P., PINSKER, R.I., PORKOLAB, M., MENEGHINI, O. & VDOVIN, V.L. 2014 Application of very high harmonic fast waves for off-axis current drive in the DIII-D and FNSF-AT tokamaks. *Nucl. Fusion* **54**, 083024.

SHIRAIWA, S., MENEGHINI, O., PARKER, R., BONOLI, P.T., GARRETT, M., KAUFMAN, M.C., WRIGHT, J.C. & WUKITCH, S. 2010 Plasma wave simulation based on a versatile finite element method solver. *Phys. Plasmas* **17**, 056119.

STIX, T.H. 1975 Fast-wave heating of a two component plasma. *Nucl. Fusion* **15**, 737–754.

STIX, T.H. 1992 *Waves in Plasmas*. Springer-Verlag.

TOLMAN, E.A. & CATTO, P.J. 2021 Drift kinetic theory of alpha transport by tokamak perturbations. *J. Plasma Phys*. **87**, 855870201.

WRIGHT, J.C., BONOLI, P.T., SCHMIDT, A.E., PHILLIPS, C.K., VALEO, E.J., HARVEY, R.W. & BRAMBILLA, M.A. 2009 An assessment of full wave effects on the propagation and absorption of lower hybrid waves. *Phys. Plasmas* **16**, 072502.